Journal of Cluster Science (2018) 29:267–279
https://doi.org/10.1007/s10876-017-1328-4

ORIGINAL PAPER

Green Synthesized Silver Nanoparticles and Their Impact on the Antioxidant Response and Histology of Indian Major Carp *Labeo rohita*, with Combined Response Surface Methodology Analysis

Chellappan Shobana[1] · Basuvannan Rangasamy[1] · Subramani Surendran[2] · Ramakrishnan Kalai Selvan[2] · Mathan Ramesh[1]

Received: 26 October 2017 / Published online: 2 January 2018

Abstract
Biosynthesis of silver nanoparticles has received considerable attention due to their cost-effective, eco-friendly and medicinal values. In this study, silver nanoparticles (Ag NPs) were synthesised using the aqueous leaf extracts of *Piper nigrum*. TEM images revealed that the particle is spherical with 20–50 nm in size. Furthermore, to evaluate the toxicity of synthesized Ag NPs, fish *Labeo rohita* were exposed to two different concentrations (2.5 µg/L as the treatment I and 5 µg/L as treatment II) for 35 days, and antioxidant parameters and histology of gill, liver and kidney were examined. A biphasic response in the activity of glutathione S-transferases (GST) was observed in gill and liver of fish. GST activity in the kidney of fish was significantly increased when compared to control group. Glutathione reductase (GR) activity in organs/tissue of fish were found to be increased while peroxidase (POD) activity was significantly decreased. Histopathological changes such as hyperplasia, proliferation of epithelial cells and fusion of lamellae were observed in both the concentrations. In liver, necrosis, nuclear degeneration and dilation of sinusoids were observed. Subsequently, the representative effects of POD activity were assessed based on the Box–Behnken Equation, 3-D contour plot and ANOVA analysis through response surface methodology analysis.

Keywords Green synthesis · Ag NPs · Oxidative stress · Histopathology · RSM analysis · *L. rohita*

Introduction

Nanoparticles (NPs) attract global responsiveness for potential application in various fields such as drug delivery, diagnostics, tissue engineering, parasitological and also in many clinical and environmental applications due to its unique physical and chemical properties [1, 2]. Specifically, metal nanoparticles have lots of concern owing to their distinctive properties. Amongst, Ag NPs have been used enormously in industries, medicine, electronic devices, textiles, consumer products, plastics, baby products, antiviral activity and also in home appliances because of their antimicrobial properties [3–6]. More than that, Ag NPs has been acknowledged with much attention among the researchers due to their prospective usage in cancer therapy [7]. The consumption of Ag NPs was approximately estimated to be around 20 metric tons per year [8]. Therefore, the demand for Ag NPs rapidly increases over a period, which leads to the exploration of numerous synthesis methods [9, 10].

Bio/green synthesis of nanoparticles has received considerable attention as they remain free from toxic and more advantageous when compared to physical and chemical synthesis [11, 12]. Moreover, it also acts as a natural capping, reducing and stabilizing agents. As a result, bio-synthesis has been anticipated as an active approach, which necessitates no sophisticated instrumentation, technical expertise, and excessive use of hazardous chemicals [13]. In this study, Ag NPs were prepared using *Piper nigrum* leaf extract as a

Electronic supplementary material The online version of this article (https://doi.org/10.1007/s10876-017-1328-4) contains supplementary material, which is available to authorized users.

✉ Mathan Ramesh
mathanramesh@yahoo.com

[1] Unit of Toxicology, Department of Zoology, Bharathiar University, Coimbatore, Tamil Nadu 641046, India

[2] Department of Physics, Bharathiar University, Coimbatore, Tamil Nadu 641046, India

reducing agent. *P. nigrum* belongs to family Piperaceae and is considered as the 'The King of Spices' [14]. The leaf contains antioxidants, vitamin A and C, alkaloids, flavonoids, organic acids and phenolic compounds which are considered as an alternative reducing and stabilizing agent for green synthesis of Ag NPs [15]. However, a limited amount of work has been reported using *P. nigrum* leaf as a reducing agent for the synthesis of nanoparticles by applying physical, chemical and biological methods [16, 17]. To the best of our knowledge, there is no report on the synthesis of Ag NPs using *P. nigrum* leaf extract as a reducing agent by microwave (MW) irradiation method. The main advantage of this method is faster, economical, simple, energy efficient and the products are pure. In this method, the energy is transferred homogenously to the material either through resonance or relaxation. Moreover, MW radiation is controlled by the law of thermodynamics and kinetics than typical reactions [18, 19].

Nevertheless, enormous use of Ag NPs results in the discharge of these particles into aquatic ecosystems and creates a severe hazardous effect on the organisms [20, 21]. Over the last few decades, quite a lot of eco-toxicity studies have been conducted to investigate the harmful effects of the Ag NPs in various organisms such as invertebrates, mosquito, algae, bacteria, albino rats, fish and human beings [22–25]. On the other hand, green synthesis of Ag NPs from leaf extract of *Malva sylvestris* and *Zornia diphylla* was found to be not toxic to non-target organisms [26–28].

Additionally, substantial evidence has been obtained that the microorganisms and plants are capable of focusing nanoparticulate materials, which lays an opportunity for the Ag NPs to accumulate in the food chain [29]. Some researchers have worked on Ag NP's toxicity in the aquatic ecosystem, predominantly on fish as a focal objective. For example, genotoxic effect of carbon nanoparticles has been reported in goldfish, *Carassius auratus* [30]. Similarly, high DNA damage has been reported in *Poecilia reticulata* and *Ceriodaphnia cornuta* upon exposure to $AgNO_3$ and Cq-AgNPs [31]. In contrast, no significant damages of DNA were observed on peripheral erythrocytes of *C. auratus* upon exposure to Ag NPs biosynthesized from neem cake up to 12 ppm [32]. A significant alteration in GST and AChE activity has been reported in *S. serrata* crabs exposed to CdS nanoparticles [33].

Since fish species considered as the best indicator of environmental pollution due to its abrupt response under various stress conditions [34–38]. Oxidative stress on fish considered as an important biomarker in the field of environmental and aquatic toxicology. Oxidative stress analysis stated that the liberation of enzymes and radicals from cellular organelles due to the exposure of NPs. It creates an inequity between the oxidants and antioxidants, which leads to accumulating excessive reactive oxygen species (ROS). It is noteworthy that increased level of ROS is an important indication of the predominant mechanism of chronic toxicity. In the normal state, free radical production and elimination are in a dynamic balance [39]. Similarly histopathological changes can be used to express the health condition of fish under chronic stress.

The present study deals with the eco-toxicological effect of green synthesised Ag NPs using *P. nigrum* leaf extract on freshwater fish *Labeo rohita*. However, a limited amount of work has been reported on green synthesised Ag NPs using other plant extracts [40, 41]. *Labeo rohita* is recognised as an excellent animal model since it is the most important species of the major Indian carp, which gives the impression to be highly economical and tolerable to general environmental conditions. Therefore, the alterations in antioxidant enzymes like GST, GR and POD enzymes estimated in the present study. Our primary aim of this present investigation is (1) to prepare Ag NPs by biosynthesis using *P. nigrum* leaf extract, (2) to investigate the response of antioxidant enzyme activity (GST, GR and POD) on *L. rohita* and (3) to analyse the histopathological alterations of the representative gill and liver. Finally, (4) the representative antioxidant activity (POD) is compared with the well-depicted response surface methodology (RSM) by making Box Behnken Equation, 3-D contour plot and ANOVA analysis.

Materials and Methods

Preparation of the Leaf Extract

Fresh and healthy *P. nigrum* (Black pepper) leaves in good physical shape were collected from areas around Coimbatore district, Tamil Nadu, India. Initially, the leaves were washed thoroughly with double distilled water to eradicate the dust particles and dried under the shades for 1 week. The collected leaves crushed into a fine powder using an electric blender and stored in a hermetic container. Subsequently, 5 gm of the powder was dispersed in 50 ml of double distilled water and boiled at a temperature of 60 °C for about 10 min in a water bath and allowed to cool for few minutes. After cooling, it was filtered using Whatman no. 1 filter paper, and the obtained extract was centrifuged further at 5000 rpm for 15 min. to take out the undesired impurities. Further, the prepared filtrate was used as a reducing and capping agent throughout the present study.

Biosynthesis of Ag NPs with Microwave Assisted Reflux Method

Analytical grade, silver nitrate ($AgNO_3$) was purchased from Himedia India Pvt. Ltd., India. For the synthesis,

1 mM of $AgNO_3$ dissolved in a 50 ml of DD water. Then, 5 ml of the leaf extract (filtrate) was added drop by drop and mixed thoroughly. The obtained golden yellow colour solution transferred into a 100 ml round bottom flask and kept in a domestic LG microwave oven (Model no: MH-4048 GW, Operating frequency − 2.45 GHz, output power − 80 W). The reaction was endorsed to proceed with the continuous 1 min on and 30 s off time. Subsequently, it was allowed to cool until it reaches the room temperature. Afterwards, the colour change was noticed (golden yellow to dark brown) signifying the formation of Ag NPs. Finally, the obtained solution was centrifuged at 20,000 rpm for 15 min and washed with distilled water and ethanol and then dried in a hot air oven about overnight.

Characterization of the Synthesised Ag Nanoparticles

The absorption spectra of as-synthesized Ag NPs were recorded using UV–Vis spectrophotometer (JascoV-550). The FT-IR spectrum was obtained using Malvon Instrument Analytical Limited and used with the samples as KBr pellets. The XPS analysis was performed through Kratos Analytical, Ultra axis instrument. The morphology of the as-synthesized Ag NPs was determined by using Transmission electron microscope (TEM) and HR-TEM (JEOL-JEM 2100). The hydrodynamic diameter and the zeta potential of the Ag NPs were characterised by dynamic light scattering (DLS) using Malvern Zetasizer Nano (Malvern Instruments Ltd, UK.) All measurements were carried out at 25 °C.

Experimental Animal and Maintenance

Labeo rohita (6–7 cm) were procured from Tamil Nadu Fisheries Development Corporation, Aliyar Fish farm, Aliyar, India. Handling and maintenance of fish were followed by the CPCSEA guidelines, Government of India. Initially, all the fish were relocated to the laboratory and acclimated to the laboratory conditions for 3 weeks. A fish meal with the composition of 3:1 ratio (groundnut oil cake and rice bran) was given every day.

Chronic Toxicity Studies

The median lethal concentration of green synthesised Ag NPs was estimated [42]. 1/10th (2.5 µg/L) and 1/5th (5 µg/L) of the LC50 range were chosen for chronic toxicity studies. After acclimatization, fish were separated into three groups (each set, 90 fishes). The first group was designated as control (toxicant free), the second group as the treatment I (2.5 µg/L) and the third group as treatment II (5 µg/L). All the groups were exposed for a period 35 days. Before starting the experiment, feeding was ceased for 48 h. Afterwards, green synthesised Ag NPs were added to the experimental medium shadowed by 1-h sonication. Proper feeding and renewal of water were carried out every day to maintain the health condition of the fish, and the nitrogenous wastes from the experimental tanks were removed.

The experiment was conducted at 7-day intervals. Initially, fish were removed from each group, and organs/tissue such as gill, liver and kidney were dissected out and washed in 0.9% saline solution. Then, the organs were weighed and homogenized with 50 mM of phosphate buffer (pH 7) containing 0.5 mM of EDTA in a glass homogenizer. The samples were centrifuged at 15,000 rpm for 20 min. The supernatants were utilized for the estimation of antioxidant enzymes such as GST, GR and POD.

Antioxidant Enzyme Activities

Assay of Glutathione S-Transferase (EC 2.5.1.14)

GST activity was measured by the method of Habig et al. [43]. Three different test tubes were taken and marked as Control, Blank and Test. To this, 1 ml of phosphate buffer and 0.1 ml of supernatant of tissue extract (gill, liver and kidney) was added, and the total volume was adjusted to manage 2.9 ml. The reaction mixture was incubated at 37 °C for 5 min followed by 0.1 ml of 30 mM of glutathione. The absorbance–wavelength was read at 340 nm against the Blank with 3 min of interval time. The reaction mixture without the tissue extract was used as a Blank.

Assay of Glutathione Reductase (GR, EC 1.6.4.2)

GR activity in the gill, liver and kidney was estimated by the method of David and Richard [44]. The assay system contained 1 ml of phosphate buffer, 0.1 ml of EDTA, 0.1 ml of sodium azide, 0.1 ml of oxidized glutathione and 0.1 ml of the supernatant of tissue homogenate and the volume was made up to 2 ml with distilled water. The tubes were incubated for 3 min at room temperature, and 0.1 ml of NADPH was added. The absorbance was read at 340 nm in a Spectrophotometer at every 15 s interval for 2–3 min. For each series of measurement, a blank was maintained with distilled water.

Assay of Peroxidase (EC 1.11.1.7)

POD activity was estimated following the method of Reddy et al. [45]. 3 ml of 0.05 mol of pyrogallol solution and 0.1–0.5 ml of supernatant of tissue homogenate was taken in a test tube, and the contents were read '0' at 400 nm. After that, freshly prepared 0.5 ml of 1% H_2O_2

was added, and the change in the absorbance was recorded for every 30 s up to 3 min.

Protein content in the gill, liver and kidney tissue was estimated by the method of Lowry et al. [46].

Histopathological Examination

Gill and liver from control, treatment 1 and treatment II were dissected out and washed in 0.9% cold saline solution and immediately fixed in 35% formalin for 24 h. After that, the fixed tissues were processed for paraffin embedding technique. Tissues were sectioned at 7 µm thickness and stained by hematoxylin and eosin. Changes were examined under light microscopy [47].

Statistical Analysis

Interpretation of data analysis was carried out using SPSS software version 20.0 via statistical package program. To compare the data, One-way ANOVA was used, after which individual means were compared using Tukey's HSD method ($P < 0.05$).

Experimental Design and Data Analysis

Usually, Central Composite Design (CCD) and Box Behnken Design (BBD) methods were used in RSM analysis [48]. In the present study, Response Surface Methodology with Box Behnken design (BBD) was applied to analyse the POD activity of the fish. Regarding this, the Ag NPs concentrations, weeks of exposure (in time), pH were selected as important factors for toxicity assessment. Totally 17 experiments were evaluated according to BBD. From this, the outcome of the results was analyzed by applying a coefficient of determination (R^2), analysis of variance (ANOVA) and response plots. Further, the polynomial equation of the BBD was prepared to fit the experimental results and categorise the appropriate model terms.

$$Y = \beta_0 + \Sigma\beta_i X_i + \Sigma\beta_i X_i^2 + \Sigma\beta_{ij} X_i X_j \quad (1)$$

Here we observed that Y is considered as a predicted response; β_0, β_i, β_j are constant regression coefficients of the model and, X_i and X_j are the independent variables.

Results and Discussion

Spectral and Morphological Analysis

Figure 1a shows the UV–Vis spectra of the Ag NPs prepared in different microwave powers (20, 40, 60, and 80%) at 5 min reaction time. At low (20%) power, the surface Plasmon Resonance (SPR) band is broad, and it was observed at 447 nm. For obtaining a sharp peak, the power was slightly increased (40%), where the SPR band gets slightly sharpened, and the peak was shifted to 438 nm. While further increasing the power (60%), a peak was obtained at 429 nm with deepened sharpness. Finally, at high power (80%), the SPR band becomes exceptionally sharper (419 nm) compared to other conditions. To further optimize the condition for the synthesis of Ag NPs, the reaction time was increased to 6 min with 80% power, the SPR band spectacles the sharp, smooth and narrow peak at 420 nm. Simultaneously, the colour of the reactant solution was changed from golden yellow to dark brown. On the other hand, increasing the reaction time (7 min) without altering the power (80%) resulted in shifting of the peak to a higher wavelength region. Therefore, it confers that the 80% power and 6 min reaction time is the optimum condition for the synthesis of Ag NPs by microwave-assisted synthesis. Further, it indicates that the microwave method is an efficient one and also its power plays a crucial role in the synthesis of Ag NPs.

It is well depicted that biosynthesised Ag NPs have greater electromagnetic absorption in the visible range due to its optical resonant property, known as Surface Plasmon Resonance [49]. The formation of the SPR band is due to the combined vibration of electrons in the metal nanoparticles. The observed difference in absorption wavelength may attribute to the number of particles and the particle size distribution in the solution. Mainly, Ag NPs acquires the free electron in abundance, which could move through conduction and valence band. In the present study, the observed strong peak at 420 nm might arise from the excitation of longitudinal Plasmon vibrations of Ag NPs present in the solution. A similar type of observations has already been reported [50, 51]. They have obtained Ag NPs using *Anacardium occidentale leaf extract* and observed the SPR at 420 nm.

For identifying the efficacy of microwave method, two different methods were adopted for the synthesis of Ag NPs including mechanical stirring and sonochemical method. For mechanical stirring, the reaction was carried out at 100 °C at different reaction periods (20, 30 and 60 min) and the obtained absorption spectra are shown in Fig. 1b. Unfortunately, no Ag peak was obtained even at a high reaction time of 1 h. Similarly, in the sonochemical method, the absorption spectra of Ag NPs were measured at different time intervals of 10, 20 30 and 60 min (Fig. 1b: inset), likewise, no Ag peak was observed at this juncture as well. That infers the importance of microwave assisted green synthesis of Ag NPs.

FT-IR analysis was carried out to find the functional groups of the potential bio-molecules present in *P. nigrum* leaf, which is responsible for the capping of the bio-

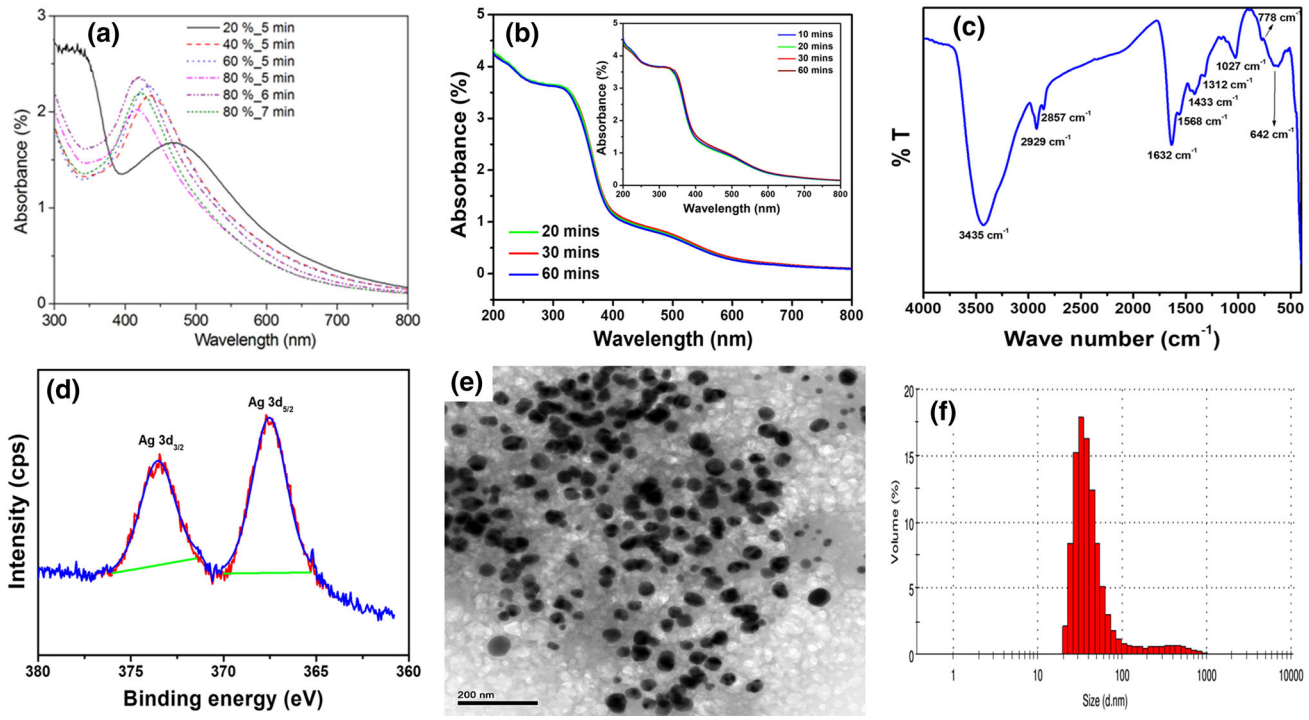

Fig. 1 UV–Vis spectra of Ag NPs prepared **a** at different microwave power and time, **b** stirring method and (inset: **b**) sonochemical method. **c** FT-IR spectrum, **d** XPS spectra of Ag 3d, **e** TEM image and **f** DLS spectrum of Ag nanoparticles prepared by microwave assisted green synthesis at 6 min reaction time

reduced Ag NPs (Fig. 1c). The following are some of the prominent peaks observed in FT-IR Ag band such as 3435, 2929, 2857, 1632, 1568, 1433, 1312 and 1027 cm^{-1}. The formation of IR band due to the C–O stretching at 1312 cm^{-1} is intense in the spectrum of Ag NPs, and this streak coincides with the results of [52]. A broad and sharp peak was observed at 3435 cm^{-1} due to the O–H stretching of the hydroxyl functional groups. The IR bands on 2929 and 2857 cm^{-1} are due to the C–H stretching of methyl, methylene or methoxy groups [53]. The IR band at 1632 cm^{-1} was due to the stretching vibration of –C=C. The noticeable band at 1433 and 1027 cm^{-1} was due to the –C–N stretching and (–C–O–C) stretching, respectively [54]. The peak at 1568 cm^{-1} was due to amide-II band. The other peaks like 778, 642 cm^{-1} was due to stretching of heterocyclic compounds like alkaloids, flavonoids present in *P. nigrum* leaf extract. The observed peaks empower the occurrence of active components of *P. nigrum* leaf extract, which acts as the reducing and capping agent for the entire duration of synthesis of Ag NPs. Thus, the result of the FTIR spectroscopic study revealed that the *P. nigrum* leaf extract could perform dual functions as both the reduction and stabilization of the Ag NPs.

X-ray photoelectron spectroscopy is considered as an essential surface-sensitive analytical technique, which is not only used for the identification of elements present in the sample but also to predict their oxidation states. Moreover, XPS measurements were employed to examine the chemical composition of Ag NPs and shown in Fig. 1d. The convoluted Ag 3d spectrum (Fig. 1d), centred at the binding energies of 367.53 and 373.56 eV, corresponding to Ag $3d_{5/2}$ and Ag $3d_{3/2}$, respectively, which is the characteristic zero oxidation state of Ag [55, 56]. Usha Rani and Rajasekharreddy [57] have reported a similar type of observations by obtaining binding energies at 368.4, and 374.4 eV corresponding to the Ag $3d_{5/2}$ and Ag $3d3_{/2}$, respectively are due to the spin–orbit splitting.

TEM images show the morphological characteristics and size of the synthesized Ag NPs. Figure 1e and Fig. S1 (a, b) shows the TEM images of the Ag NPs prepared at 6 min. Here we could notice that the particles were the spherical shape and uniformly distributed in size ranging from 40 nm. Moreover, each nanoparticle remains discrete without forming any agglomeration. Fig. S1(c) shows the particle size histogram of silver NPs; it depicts that the maximum number of particles were lying in the range of 30–40 nm. The HRTEM image (Fig. S1 d, e) shows the well-defined lattice fringes with an inter-planar spacing of 0.937 nm, which corresponds to the (331) plane of Ag NPs. The observed high-quality fringes indicate the formation of

highly crystalline nature of Ag NPs. Further, the SAED pattern revealed the formation of ring pattern that corroborates the polycrystalline nature of silver (Fig. S1e). The calculated d-spacing values from the inner to outer ring is 0.2414, 0.2149, 0.1533, 0.1324 and 0.1212 nm corresponding to the (111), (200), (220), (311) and (222) planes, respectively. The diffraction rings also suggested that the prepared Ag NPs were polycrystalline nature.

Further, to identify the size of the nanoparticles, the dynamic light scattering (DLS) measurement was carried out. It is a technique for characterising the size of colloidal dispersions through the illumination of a suspended particles or molecules, which undergoing Brownian motion by a laser beam. The obtained size distribution of Ag NPs is shown in Fig. 1f. From this study, it was observed that the Ag NPs prepared with *P. nigrum* leaf extract was around 20–100 nm, but the size of the maximum number of particles was around 30–40 nm. Usually, the size and shape of the metal nanoparticles were influenced by some factors including pH, precursor concentration, reductant concentration, time of incubation, temperature as well as the method of preparation. Therefore, DLS study confirms that the prepared Ag NPs are nanoscale in size.

Antioxidant Enzyme Responses

The response of antioxidant enzyme activities including GST, GR and POD were assessed for 35 days from the gill, liver and kidney of the Indian major carp *L. rohita*, and the corresponding results are shown in Figs. 2, 3 and 4. It infers that significant variations were observed in all the organs when compared with their control group. During chronic exposure, GST activity (Fig. 2a) in gill was significantly decreased up to 21st day in both the treatments. A maximum percent decrease (44.79%) was witnessed during treatment II at the end of the 7th day. In contrast, GST activity was found to be progressively increased to a considerable extent ($P < 0.05$) at the end of the 35th day in both the treatments. A maximum activity (90.77%) was noticed at the end of the 35th day in treatment II. On the contrary, a significant reduction was observed in liver (Fig. 2b) at the end of the 7th and 14th day in both the treatments. A maximum percent increase of 74.43 and 118.41% was noticed treatment I and II at the end of the 35th day, respectively. On the other hand, GST activity in the kidney (Fig. 2c) was gradually increased in both the treatments throughout the study period showing a maximum percent increase of 116.58 and 198.86% at the end of the 28th day in treatment I and II, respectively.

In general, GST is an enduring enzyme that participates in the detoxification of a wide variety of xenobiotics and also plays a part in the waning of free radical damages in erythrocytes. A substantial decrease in the GST activity

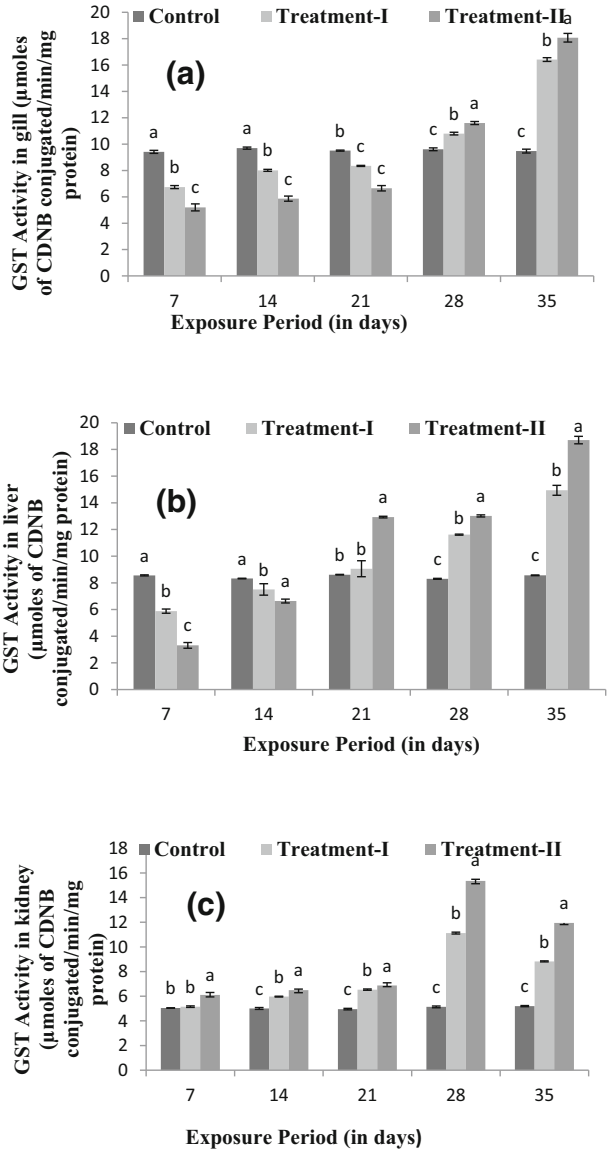

Fig. 2 Changes in the antioxidant enzyme, GST (**a** Gill, **b** liver, **c** kidney) in a freshwater fish *Labeo rohita* treated with Ag NPs for 35 days. Results are presented as mean ± SE. Bars with same letters are not significantly different ($P > 0.05$) according to DMRT

was observed in *Cyprinus carpio* fingerlings exposed to tebuconazole [58]. On the other hand, GST activity in the liver was increased, when rainbow trout was treated with propiconazole for 20 and 30 days [59]; but in the case of gill, GST activity was found to be decreased. In the present study, the observed increase in GST activity in the kidney of fish may be one of the adaptive mechanisms of mild oxidative stress induced by the Ag NPs. A similar increase in GST activity has been reported in *S. serrata* upon exposure to CdS nanoparticles indicating that oxidative stress produced by CdS nanoparticles may be the possible reason [33]. However, the decrease in the GST activity of

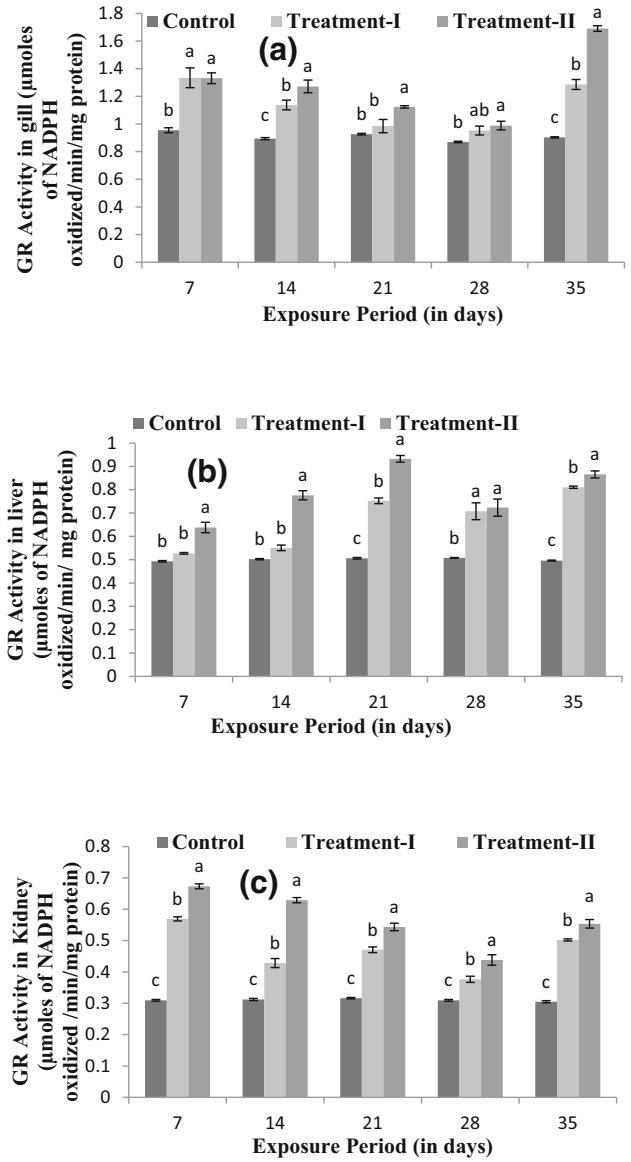

Fig. 3 Changes in the antioxidant enzyme, GR (**a** Gill, **b** liver, **c** kidney) in a freshwater fish *Labeo rohita* treated with Ag NPs for 35 days. Results are presented as mean ± SE. Bars with same letters are not significantly different ($P > 0.05$) according to DMRT

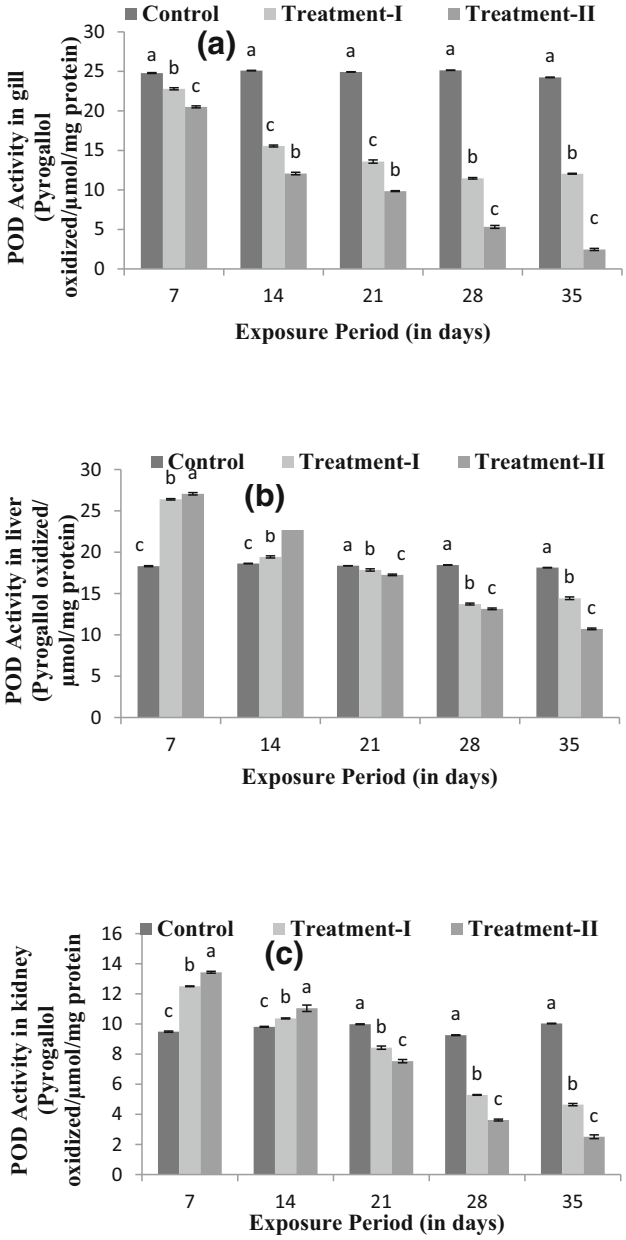

Fig. 4 Changes in the antioxidant enzyme, POD (**a** Gill, **b** liver, **c** kidney) in a freshwater fish *Labeo rohita* treated with Ag NPs for 35 days. Results are presented as mean ± SE. Bars with same letters are not significantly different ($P > 0.05$) according to DMRT

the gill and liver may be due to the severe oxidative stress results in a rise to the exhaustion of GSH [60, 61].

Glutathione reductase (GR) is an auxiliary enzyme in an antioxidant defence; GR reduces the oxidized glutathione (GSSG) to its active form of reduced glutathione (GSH) action [62]. Alterations in the glutathione reductase (GR) activity in gill, liver and kidney are presented in Fig. 3a–c. Glutathione reductase (GR) activity in gill (Fig. 3a) has shown a significant elevation ($P < 0.05$) throughout the study period. In this study, a maximum GR activity in gill was noticed at the end of the 35th day in treatment I (42.32%) and treatment II (+ 87.09%). Similarly, in the liver, GR activity (Fig. 3b) was intensely increased during the chronic exposure and showed a maximum increase of + 63.39 and + 84.24% in treatment I (on 35th day) and treatment II (on 28th day), respectively. In contrast, GR activity in kidney was significantly ($P < 0.05$) increased at the end of the 7th day in both the treatments (Fig. 3c). The statistical analysis revealed that the substantial level of 5% ($P < 0.05$) was acquainted with all the cases.

Glutathione reductase is found in the cells of the organisms, which catalyzes the reduction of oxidized glutathione (GSSG) to glutathione (GSH). Besides, it is

entangled in the glutathione redox cycle that maintains sufficient levels of reduced cellular GSH [63–67]. GR activity in gill cells of *Anguilla* exposed to iron oxide nanoparticles significantly elevated at the end of 72 h [67]. Similarly, increased level of GR activity was observed, when the fish *C. auratus* treated with manganese for 3 days [64], fish exposed to MRC-5 cells of iron oxide nanoparticles [65] and in rainbow trout exposed to Cu nanoparticles [66]. In the present study, GR activity was noticeably increased in gill, liver and kidney throughout the study period (35 days). The prominent level of GR activity may be due to the adaptive response of the cells to defend the oxidative stress generated by the exposure of Ag NPs [63].

POD activity of fish exposed to Ag NPs is depicted in Fig. 4a–c. When compared with the control group, gill POD activity was gradually decreased at the end of the 35th day, and a maximum decrease of − 89.83% was noted for treatment II. It can be seen that the enzyme POD activity in liver (Fig. 4a) was increased at the end of 7 and 14 days with the maximum increase of + 47.83% for treatment I. Likewise, a major reduction of POD activity in liver (Fig. 4b) was revealed at the end of 21, 28 and 35th day in both the treatments. However, the perceived maximal decrease rate of − 40.89% was noticed at the end of the 35th day in treatment II. A biphasic trend was observed in kidney (Fig. 4c) during the investigation of both the treatments when compared with their control group ($P < 0.05$). Nevertheless, in most of the days, the enzyme POD activity was identified as decreasing with a maximal decrease of − 74.94% at the end of the 35th day in treatment II.

It is well known that the POD is considered as a key enzyme like CAT, in an antioxidant defence system which converts the obtained free radicals H_2O_2 to water and oxygen. Also, the enzyme POD comes under the category of the first level of defence against the oxidative toxicity at the cellular level [68, 69]. A significant decrease in POD activity was observed in gill and liver of fish *Oreochromis mossambicus* exposed to nickel nanoparticles [69]. Govindasamy and Rahman [39] reported the elevated level of POD activity in different tissues of the fish *O. mossambicus* exposed to Ag nanoparticles. Likewise, in the present study also POD activity in the gill was significantly increased during the study period. However, in the case of liver and kidney, a biphasic trend of POD activity was observed throughout the study period.

In general, silver has the capability of high reactivity and great adsorption of the biologic particles. The physicochemical itineraries like sedimentation, aggregation of NPs postures as the crucial factors that determine the behaviour and fate of NPs in the aquatic environment [70]. The exposure media has the physicochemical features like salinity, ionic strength, pH, divalent cations, and organic material that are the most noteworthy parameters unsettling the strength of the dispersed nanoparticles in an aqueous environment [71]. The primary mechanism of the Ag NPs toxicity may involve adhesion to membranes, shifting their properties such as permeability or ion transport shadowed by disturbances in the cellular phosphate management, induction of DNA synthesis, creating a collapse in the proton pump, alluring ROS generation, instigating the DNA damage, breaking of H bonding, denaturation of ribosomes, degradation of lipopolysaccharide molecules, and inactivation of proteins and enzymes by bonding on active sites (especially on SH groups) [19, 72].

Moreover, the Ag ions released from the surface of NPs can interact with the thiol groups, and proteins are demobilizing enzymes, which can restrict the accessibility of these molecules for ROS neutralization resulting in oxidant-mediated response to ROS [70, 73]. Apart from these, different factors also responsible for the toxicity of Ag NPs like as size, surface area, shape, chemical composition and surface charges [74]. The alterations of ROS results in lipid peroxidation, protein oxidation, modulation of gene expression, changes in redox status as cellular effects, and some diseases and premature ageing as effects in the stages of the organism [75].

Histopathological Studies

The photomicrographs of the histopathological images of the representative organs of gill and liver are given in Fig. 5a–f. Compared with control group, various histopathological changes were identified in the gill and liver tissue of *L. rohita* exposed to Ag NPs at the end of 35th day. Gills are recognized as the key organ, which involved in respiration, osmotic balance and nitrogenous elimination of waste materials. At lower concentration of Ag NPs (Fig. 5b), degeneration of primary and secondary lamellae, a fusion of secondary lamellae and curling of lamellae were observed. At higher concentration (Fig. 5c), the severity of lamellar degeneration, the proliferation of epithelial cells, severe congestion of secondary lamellae and gill edema were identified when compared with control group (Fig. 5a). The above said changes might affect the osmoregulation and respiratory stress to the fish. Griffitt and his group [76] have already reported a similar type of observations for the gill tissue of zebrafish exposed to Ag NPs. Likewise, gill stimulation and increased mucus secretion have been reported in *P. reticulata* and *C. cornuta* when exposed to green synthesized Ag NPs [31].

It is well known that liver is the primary organ and important site for storage and glycogen synthesis, which also considers as an essential metabolic centre for detoxification of chemicals and glucose manufacture and storage mechanism. While treating with a low concentration of Ag

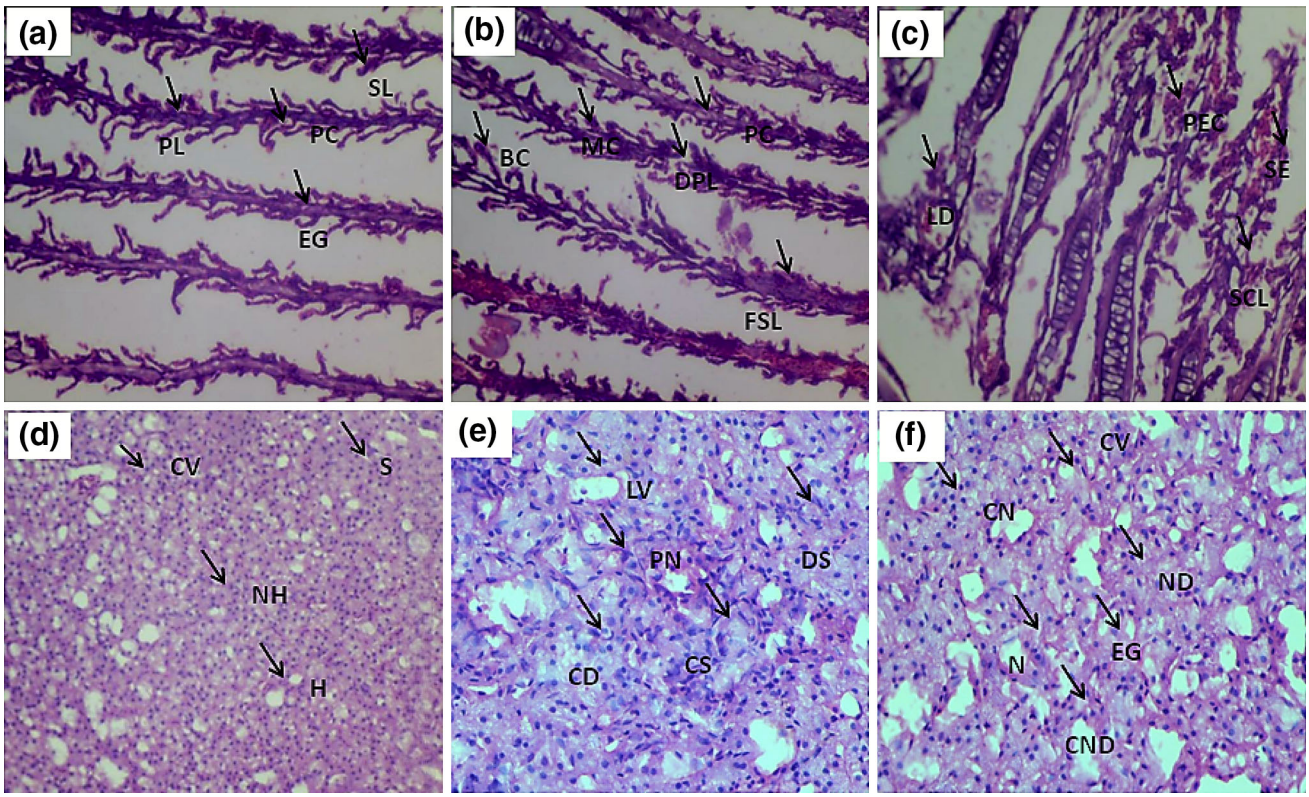

Fig. 5 Light micrographs of sections through gill (**a**–**c**) and liver (**d**–**f**) of *Labeo rohita* showing histological structure (**a**, **d** control; **b**, **e** treatment 1; **c**, **f** treatment 2) after the treatment of Ag NPs for 35 days. *PL* primary lamellae, *SL* secondary lamellae, *PC* pillar cells, *EG* erythrocyte granules, *BC* bavement cells, *MC* mucous cells, *DPL* degeneration of primary lamellae, *FSL* fusion of secondary lamellae, *LD* lamellar degeneration, *PEC* proliferation of epithelial cells, *SCL* severe congestion of secondary lamellae, *SE* small edema in gill tissue (200X), *LV* lipid vacuolization, *H* hypertrophy, *S* sinusoids, *CD* cytoplasmic degeneration, *ND* nuclear degeneration, *CV* cytoplasmic vacuolation, *DS* dilated sinusoids, *CND* cytoplasmic and nuclear degeneration, *PN* pycnotic nuclei, *CS* cloudy swelling, *N* necrosis, *CN* condensation of the nuclei (400X)

NPs, lipid vacuolation, pycnotic nuclei, cloudy swelling of hepatocytes, dilated sinusoids and cytoplasmic degeneration was examined (Fig. 5e). Similarly, severe necrosis, nuclear and cytoplasmic degeneration, condensation of nuclei, melanomacrophage aggregates were noticed at higher concentration (Fig. 5f), when compared with control group (Fig. 5d). A similar type of pathological liver alterations was also noticed in zebrafish (*Danio rerio*) exposed to Ag NPs [77].

Response Surface Methodology (RSM) Analysis

In the current scenario, the development of modern statistical analytical methods has encouraged to analyze the toxicity assessment of nanoparticles [78–80]. It is well known that the RSM analysis implicates many independent variables and their interactions triggering the desired responses [81]. In addition to the experimental strategy, RSM can also assist the scientists to prove if any alterations in the independent factors are produced with a statistically significant variation in the observed response [82, 83]. In this study, BBD was applied to analyze the toxicity concentration of green synthesized Ag NPs, the essential time duration and pH value. The parameters used for the experimental design is given in Table S1. The significant importance of RSM is the least number of experimental trials are preferred to analyze various parameters and their interactions. This characteristic feature is known as the response and is usually evaluated on a continuous scale, which represents an essential function of the systems [84].

The ANOVA for surface quadratic regression model explained that it was a more significant model evident from the F test and the F value is 2727.86, and the probability was < 0.0001, and this data indicates that the models were highly significant (Table 1). Values of "Probability $> F$" less than 0.0500 indicate model terms are worth mentioning. Here, A, B, AB, A^2, B^2, C^2 are renowned as model terms. Values greater than 0.1 indicate the model terms are not influential. There was only a 0.01% chance that an F value could occur due to noise. From this study, the predicted R^2 is 0.9954 and the adjusted R^2 value is 0.9993, which is in good agreement with the attuned R^2 and the

Table 1 Analysis of variance (ANOVA) for the response surface quadratic model

Source	df	SS			*F* value			Prob > *F*		
		Gill	Liver	Kidney	Gill	Liver	Kidney	Gill	Liver	Kidney
Model	9	735.09	327.46	193.51	473.45	36.85	2727.86	< 0.0001 significant	< 0.0001 significant	< 0.0001 significant
A-Week	1	668.32	307.52	177.19	3873.98	311.49	22,479.97	< 0.0001	< 0.0001	< 0.0001
B-Ag Concentration	1	12.60	2.24	1.19	73.04	2.27	150.44	< 0.0001	0.1760	< 0.0001
C-pH	1	2.29	0.33	1.125E−004	13.27	0.34	0.014	0.0083	0.5801	0.9083
AB	1	0.92	4.77	2.36	5.34	4.84	298.93	0.0541	0.0638	< 0.0001
AC	1	0.19	1.60	0.000	1.12	1.62	0.000	0.3246	0.2436	1.0000
BC	1	2.02	0.000	2.250E−004	11.69	0.000	0.029	0.0112	1.0000	0.8706
A^2	1	41.51	9.16	6.66	240.64	9.28	844.71	< 0.0001	0.0187	< 0.0001
B^2	1	1.57	0.44	1.10	9.08	0.44	138.94	0.0196	0.5267	< 0.0001
C^2	1	3.01	1.63	3.86	17.43	1.65	489.74	0.0042	0.2395	< 0.0001
Residual	7	1.21	6.91	0.055						
Lack of Fit	3	1.21	6.91	0.055						
Pure Error	4	0.000	0.000	0.000						
Cor Total	16	736.30	334.37	193.57						

differences between these two are less than 0.2. This result may indicate better concurrence of the model with the experimental data, thus mitigating the validity of the response model and the necessity for optimal conditions. In connection with this above testimonials, 3D plots of graphical representations were created which is given in Fig. 6. Mainly, the results of this study indicated that POD enzyme activity play a pivotal role in antioxidant response because it is involved in the first line of the defence system.

The outcome of this study revealed that there was a significant relationship between the metal concentration, time duration (week) joint with pH value and enzyme activity (POD) of gill, liver and kidney for toxicity assessment. The model predicted a maximum POD activity of 22.35 µmol/mg protein in a gill appeared at first week of 2.5 µg/L of Ag NPs exposed concentrations with a pH of 7.5. Like that, the encroachment of enzyme POD activity in a liver of 27.06 µmol/mg protein appeared at first week of 5 µg/L of Ag NPs treated concentrations with a pH of 7.5. Similarly, the results obtained from the model predicted an upgraded level of enzyme (POD) activity in the kidney of 13.43 µmol/mg protein appeared at first week of 5 µg/L of Ag NPs treated group with a pH of 7.0. During this study, the predicted model was validated, and the experiments were carried out using the same conditions as mentioned. The intended value predicted from the model was in good concordance with the results achieved from the experiments.

The coefficients of the regression equation were calculated and the regression equations for gill (Eq. 2), liver (Eq. 3) and kidney (Eq. 4) are as follows:

$$Y = 15.55 - 9.14 \times A - 1.25 \times B - 0.54 \times C + 0.48 \times AB + 0.22 \times AC + 0.71 \times BC - 3.14 \times A^2 - 0.61 \times B^2 - 0.84 \times C^2 \quad (2)$$

$$Y = 17.85 - 6.20 \times A - 0.53 \times B + 0.20 \times C + 1.09 \times AB + 0.63 \times AC + 0.00 \times BC + 1.47 \times A^2 + 0.32 \times B^2 - 0.62 \times C^2 \quad (3)$$

$$Y = 6.50 - 4.71 \times A - 0.38 \times B + 3.750 \times 10^{-3} \times C - 0.77 \times AB + 0.00 \times AC - 7.5 \times 10^{-3} \times BC + 1.26 \times A^2 + 0.51 \times B^2 + 0.96 \times C^2 \quad (4)$$

Here Y stands for POD enzyme activity in a gill, liver and kidney. A meant for a time duration (in weeks), B meant for Ag concentration, C is water pH respectively.

Similarly, Guo and his group [80] analyzed this RSM model in the field of toxicology using organophosphorus pesticide dimethoate on rotifers. Giloni-Lima [85] reported that the non-linear polynomial model was employed in the simulation to afford a better understanding of the concentration of the toxicant and time interaction in aquatic toxicity, which also corroborated with our results. To the best of our knowledge, there is no RSM analysis about the Ag NPs toxicity associated with the antioxidant enzyme (POD) activity.

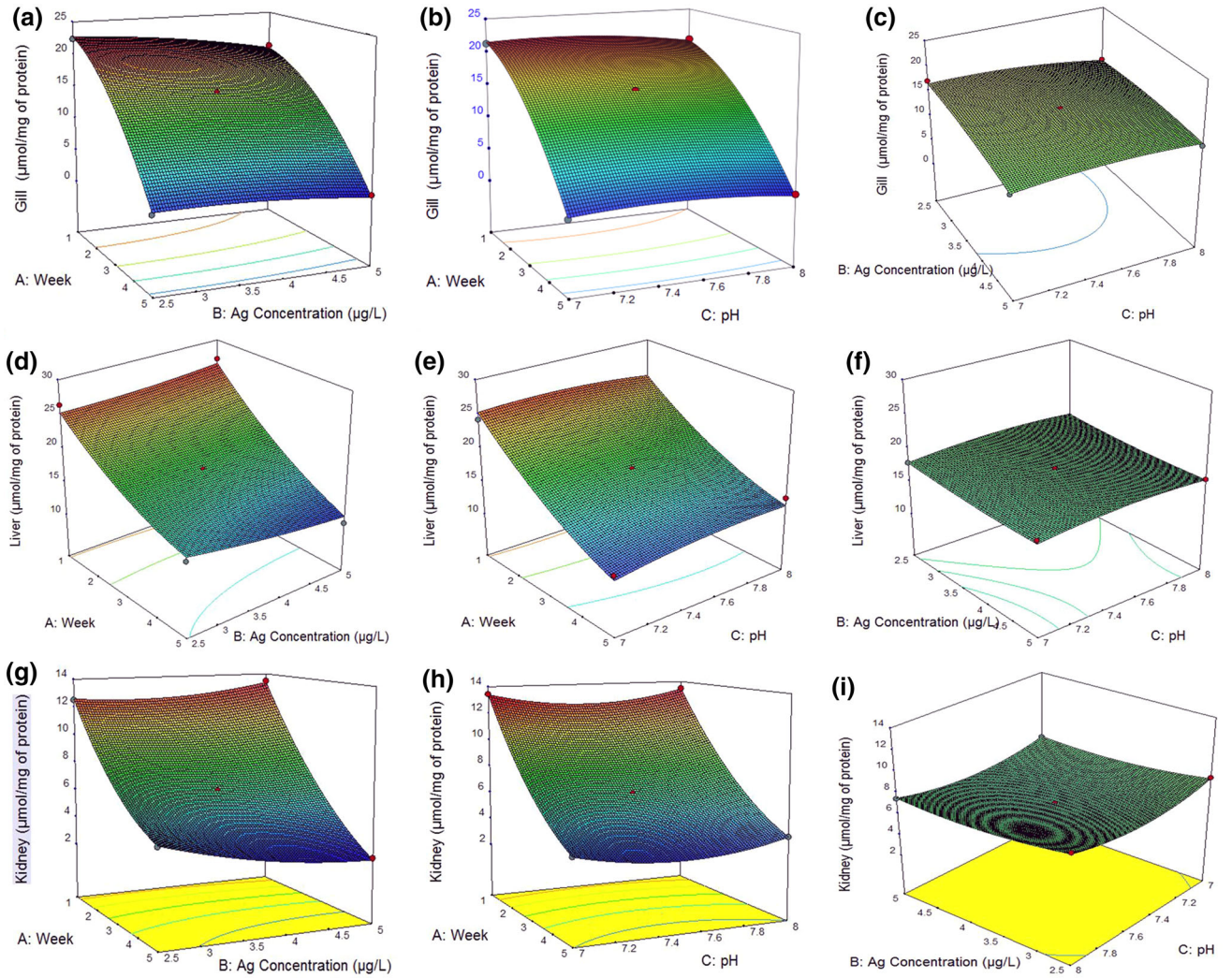

Fig. 6 3D plots of combined effects of three variables on POD enzyme activity in gill (**a**–**c**), liver (**d**–**f**) and kidney (**g**–**i**)

Conclusions

Using microwave assisted reflux method; Ag NPs were efficiently synthesized using *P. nigrum* leaf extract as reducing agent. Different microwave powers were utilized in this study, demonstrates that power plays a vital role in synthesizing Ag NPs. The obtained SPR band at 420 nm through UV–visible spectra corroborated the formation of Ag NPs. TEM and HRTEM images confirmed that the prepared Ag NPs were a spherical shape with polycrystalline nature. Subsequently, the antioxidant responses (GST, GR and POD) of Indian major carp *L. rohita* was studied using Ag NPs at two different sublethal concentrations. The corresponding changes were estimated using various organs like gill, liver and kidney. It revealed that the Ag NPs produces an alteration of antioxidant enzyme activity and oxidative stress in the experimental animal *L. rohita.* Further, the RSM analysis emphasised that the assessment of predicted values is good agreement with the enzyme POD activity in gill, liver and kidney (F-2727.86, $P < 0.0001\%$). The estimated result of this study indicates that the data is beneficial for the evaluation of environmental monitoring assessment and also for the safe design of Ag NPs and their potential applications. However, further studies are needed to carry out the bioaccumulation of Ag NPs in tissues and compare the toxicity with their ions.

References

1. G. Benelli and C. M. Lukehart (2017). *J. Clust. Sci.* **28**, 1–2.
2. G. Benelli (2018). *Acta Trop.* **178**, 73–80.
3. J. J. Wu, G. J. Lee, Y. S. Chen, and T. L. Hu (2012). *Curr. Appl. Phys.* **12**, S89–S95.
4. E. Lombi, E. Donner, K. G. Scheckel, R. Sekine, C. Lorenz, N. V. Goetz, and B. Nowack (2014). *Chemosphere* **111**, 352–358.

5. B. Nowack, K. F. Krug, and M. Height (2011). *Environ. Sci. Technol.* **45**, 1177–1183.
6. R. M. S. T. Azarudeen, M. Govindarajan, A. Amsath, U. Muthukumaran, and G. Benelli (2017). *J. Clust. Sci.* **28**, 179–203.
7. J. Dobson (2006). *Nanomedicine* **1**, 31–37.
8. SCENIHR (Scientific Committee on Emerging and Newly Identified Health Risk) (2014). European Commission, Luxembourg.
9. S. Shankar and J. W. Rhim (2015). *Carbohydr. Polym.* **130**, 353–363.
10. B. Paul, B. Bhuyan, D. D. Purkayastha, and S. S. Dhar (2016). *J. Photochem. Photobiol. B* **154**, 1–7.
11. G. Benelli, F. Maggi, R. Pavela, et al. (2017). *Environ. Sci. Pollut. Res* 1–23.
12. G. Benelli, R. Pavela, F. Maggi, R. Petrelli, and M. Nicoletti (2017). *J. Clust. Sci.* **28**, 3–10.
13. V. Kumar, D. K. Singh, S. Mohan, and S. H. Hasan (2016). *J. Photochem. Photobiol. B* **155**, 39–50.
14. G. Nahak and R. K. Sahu (2011). *J. Appl. Pharma. Sci.* **01**, 153–157.
15. A. K. Tripathy, D. C. Jain, and S. Kumar (1996). *J. Med. Aromat. Plant Sci.* **18**, 302–321.
16. N. Jayaprakash, J. J. Vijaya, L. J. Kennedy, K. Priadharsini, and P. Palani (2014). *Mater. Lett.* **137**, 358–361.
17. B. Mohapatra, S. Kuriakose, and S. Mohapatra (2015). *J. Alloys Compd.* **637**, 119–126.
18. K. D. Raner, C. R. Strauss, F. Vyskoc, and L. Mokbel (1997). *J. Org. Chem.* **58**, 950.
19. S. A. Galema (1997). *Chem. Soc. Rev.* **26**, 233.
20. P. V. Luoma (2008). *Eur. J. Clin. Pharmacol.* **64**, 841–850.
21. S. J. Klaine, P. J. J. Alvarez, G. E. Batley, T. F. Fernandes, R. D. Handy, D. Y. Lyon, S. Mahendra, M. J. McLaughlin, and J. R. Lead (2008). *Environ. Toxicol. Chem.* **27**, 1825–1851.
22. C. Carlson, S. M. Hussain, A. M. Schrand, L. K. Braydich-Stolle, K. L. Hess, R. L. Jones, and J. J. Schlager (2008). *J. Phys. Chem. B* **112**, 13608–13619.
23. P. Gopinath, S. K. Gogoi, A. Chattopadhyay, and S. S. Ghosh (2008). *Nanotechnology* **19**, 075104.
24. E. I. Mahdy, T. A. S. Eldin, H. S. Alyd, F. F. Mohammed, and M. I. Shaalan (2015). *Exp. Toxicol. Pathol.* **67**, 21–29.
25. M. Govindarajan, S. L. Hoti, M. Rajeswary, and G. Benelli (2017). *Parasitol. Res.* **115**, 2685–2695.
26. M. Govindarajan, M. Rajeswary, U. Muthukumaran, S. L. Hoti, H. F. Khater, and G. Benelli (2016). *J. Photochem. Photobiol. B: Biol.* **161**, 482–489.
27. M. Govindarajan, H. F. Khater, C. Panneerselvam, and G. Benelli (2016). *Res. Veter. Sci.* **107**, 95–101.
28. M. Govindarajan and G. Benelli (2016). *Parasitol. Res.* **115**, 925–935.
29. G. Oberdörster, E. Oberdörster, and J. Oberdörster (2005). *Environ. Health. Perspect.* **113**, 823–839.
30. K. Murugan, D. Nataraj, P. Madhiyazhagan, et al. (2016). *Parasitol. Res.* **115**, 1071–1083.
31. R. Ishwarya, B. Vaseeharan, S. Shanthi, et al. (2017). *J. Clust. Sci* **28**, 519–527.
32. B. Chandramohan, K. Murugan, C. Panneerselvam, et al. (2016). *Parasitol. Res.* **15**, 1015–1025.
33. V. Sujitha, K. Murugan, D. Dinesh, et al. (2017). *Aquat. Toxicol.* **188**, 100–108.
34. P. V. Asharani, N. G. Serina, M. H. Nurmawati, Y. L. Wu, Z. Gong, and S. Valiyaveettil (2008). *J. Nanosci. Nanotechnol.* **8**, 3603–3609.
35. Y. J. Chae, C. H. Pham, J. Lee, E. Bae, J. Yi, and M. B. Gu (2009). *Aquat. Toxicol.* **94**, 320–327.
36. M. S. Khan, F. Jabeen, N. A. Qureshi, M. S. Asghar, M. Shakeel, and A. Noureen (2015). *J. Biodivers. Environ. Sci.* **6**, 211–227.
37. K. S. Rajkumar, N. Kanipandian, and R. Thirumurugan (2016). *Appl. Nanosci.* **6**, 19–29.
38. M. S. Khan, N. A. Qureshi, and F. Jabeen (2017). *Appl. Nanosci.* **7**, 167–179.
39. R. Govindasamy and A. A. Rahuman (2012). *J. Environ. Sci.* **24**, 1091–1098.
40. V. Vignesh, K. F. Anbarasi, S. Karthikeyeni, G. Sathiyanarayanan, P. Subramanian, and R. Thirumurugan (2013). *Colloids. Surf A. Physicochem. Eng. Asp.* **439**, 184–192.
41. C. Krishnaraj, L. Stacey, B. Harper, and S. Yun (2016). *J. Hazard. Mater.* **301**, 480–491.
42. D. J. Finney, 3rd Ed (Charles Griffin, London, 1978).
43. W. H. Habig, M. J. Pabst, and W. B. Jakobi (1974). *J. Biol. Chem.* **249**, 7130–7139.
44. M. David and J. S. Richard (1983). J Mariare GB (Ed) Verlag Chemic Weinheina Dec Field Beach Florida based P, 358.
45. K. P. Reddy, S. M. Subhani, P. A. Khan, and K. B. Kumar (1995). *Plant. Cell. Physiol.* **26**, 987–994.
46. O. H. Lowry, N. J. Rosebrough, A. L. Farr, and R. J. Randall (1951). *J. Biol. Chem.* **193**, 265–275.
47. D. Bancroft and A. Stevens (Churchill Livingstone, Edinburgh, London, 1982), p. 262.
48. G. Hanrahan and K. Lu (2006). *Crit. Rev. Anal. Chem.* **36**, 141–151.
49. K. Vijayarahavan, S. P. Kamala Nalini, N. Udaya Prakash, and D. Madhankumar (2012). *Colloids Surf. B* **94**, 114–117.
50. D. S. Sheny, J. Mathew, and D. Philip (2011). *Spectrochim. Acta. Part A* **79**, 254–262.
51. A. Annamalai, S. T. Babu, N. A. Jose, D. Sudha, and C. V. Lyza (2011). *World Appl. Sci. J.* **13**, 1833–1840.
52. D. Philip, C. Unni, S. Aromal, and V. K. Vidhu (2011). *Spectrochim. Acta. Part A* **78**, 899–904.
53. V. Kathiravan, S. Ravi, and S. Ashokkumar (2014). *Spectrochim. Acta. Part A* **130**, 116–121.
54. P. K. Kumar, W. Paul, and C. P. Sharma (2012). *J. BioNanoSci.* **2**, 144–152.
55. L. Salido, D. C. Lim, and Y. D. Kim (2005). *Surf. Sci.* **588**, 6.
56. Y. Tian, F. Wang, Y. Liu, F. Pang, and X. Zhang (2014). *Electrochim. Acta* **146**, 646–653.
57. P. Usha Rani and P. Rajasekharreddy (2011). *Colloids Surf. A* **389**, 188–194.
58. C. Toni, D. Ferreira, L. C. Kreutz, V. L. Loro, and L. G. Barcellos (2011). *Chemosphere* **83**, 579–584.
59. Z. H. Li, V. Zlabek, P. Li, R. Grabic, J. Velisek, J. Machova, and T. Randak (2010). *Ecotoxicol. Environ. Saf.* **73**, 1391–1396.
60. J. F. Zhang, H. Liu, Y. Y. Sun, X. R. Wang, J. C. Wu, and Y. Q. Xue (2005). *Environ. Toxicol. Pharmacol.* **19**, 185–190.
61. A. Malarvizhi, M. Saravanan, R. K. Poopal, J. H. Hur, and M. Ramesh (2017). *Water Air Soil Pollut.* **228**, 310.
62. V. I. Lushchak (2014). *Chem. Biol. Interact.* **224C**, 164–175.
63. D. Dolphin, R. Poulson and O. Avramovic, vol. III (Part A and Part B) (Wiley, New York, 1989).
64. S. Paraschiv, M. C. Munteanu, D. Dinu, M. R. Luca, M. Costache, C. Tesio, and A. Dinischiotu (2006). *Rev. Roum. Chim.* **51**, 1175–1179.
65. M. Radu, S. Petrache, A. I. Serban, D. Dinu, A. Hermenean, C. Sima, and A. Dinischiotu (2010). *Acta. Biochim. Pol.* **57**, 355.
66. M. Eyckmans, N. Celis, N. Horemans, R. Blust, and G. De Boeck (2011). *Aquat. Toxicol.* **103**, 112–120.
67. K. Srikanth, I. Ahmad, J. V. Rao, T. Trindade, A. C. Duarte, and E. Pereira (2014). *Comp. Biochem. Physiol. Part C* **162**, 7.
68. Y. Z. Fang and R. L. Zheng (Science Press, Beijing, 2002), p. 122.
69. C. Jayaseelan, A. A. Rahuman, R. Ramkumar, P. Perumal, G. Rajakumar, A. VishnuKirthi, T. Santhoshkumar, and S. Marimuthu (2014). *Ecotoxicol. Environ. Saf.* **107**, 220–228.

70. E. Navarro, F. Piccapietra, B. Wagner, F. Marconi, R. Kaegi, N. Odzak, L. Sigg, and R. Behra (2008). *Environ. Sci. Technol.* **42**, 8959–8964.
71. L. V. Stebounova, E. Guio, and V. H. Grassian (2011). *J. Nanopart. Res.* **13**, 233–244.
72. A. Kedziora, K. Gorzelanczyk, and G. B. Płoskonska (2013). *Biol. Int.* **53**, 67–76.
73. I. M. Garrido, S. Perez, and J. Blasco (2015). *Mar. Environ. Res.* **111**, 60–73.
74. A. Hedayathi, H. Kolangi, A. Jahanbakhshi, and E. F. Shalu (2012). *Bulg. J. Vet. Med.* **15**, 172–177.
75. A. Slaninova, M. Smutna, H. Modra, and Z. Svobodova (2009). *Neuro. Endocrinol. Lett.* **30**, 2–12.
76. R. J. Griffitt, K. Hyndman, N. D. Denslow, and D. S. Barber (2009). *Toxicol. Sci.* **107**, 404–415.
77. G. P. Devi, K. B. A. Ahmed, B. S. Sai Varsha, M. K. N. Shrijha, K. K. S. Lal, V. Anbazhagan, and R. Thiagarajan (2015). *Aquat. Toxicol.* **158**, 149–157.
78. T. W. Schultz and M. T. D. Cronin (1999). *J. Chem. Inf. Comput. Sci.* **39**, 304-309.
79. S. Ren (2003). *J. Chem. Inf. Comput. Sci.* **43**, 1679–1687.
80. R. Guo, X. Ren, and H. Ren (2012). *J. Hazard. Mater.* **237**, 270–276.
81. M. Khosravi and S. Arabi (2016). *Water Sci. Technol.* **74**, 343–352.
82. C. Sudhakar, K. Selvam, M. Govarthanan, B. Senthilkumar, A. Sengottaiyan, M. Stalin, and T. Selvankumar (2015). *J. Genet. Eng. Biotechnol.* **13**, 93–99.
83. M. Govarthanan, R. Mythili, T. Selvankumar, S. Kamala-Kannan, D. Choi, and Y. Chang (2017). *Biotechnol. Bioproc. Eng.* **22**, 186–194.
84. K. P. Gopinath, K. Muthukumar, and M. Velan (2010). *J. Chem. Eng.* **157**, 427–433.
85. P. C. Giloni-Lima, D. Delello, M. L. M. Cremonez, V. A. Eler, M. N. Lima, and E. L. G. Espindola (2010). *Ecotoxicology* **19**, 1095–1101.